

# Applications of $^{129}\text{Xe}$ and PFG NMR techniques on adsorption and diffusion of molecular sieve materials

Shushu Gao<sup>a,b</sup>, Jiamin Yuan<sup>d</sup>, Fangxiu Ye<sup>b,c,f</sup>, Zhiqiang Liu<sup>e</sup>, Anming Zheng<sup>d,e,\*</sup>, Shutao Xu<sup>b,c,f,\*</sup>

<sup>a</sup> Sinopec Beijing Research Institute of Chemical Industry, Beijing 100013, China

<sup>b</sup> National Engineering Research Center of Lower-Carbon Catalysis Technology, Dalian Institute of Chemical Physics, Chinese Academy of Sciences, Dalian 116023, China

<sup>c</sup> State Key Laboratory of Catalysis, Dalian Institute of Chemical Physics, Chinese Academy of Sciences, Dalian 116023, China

<sup>d</sup> State Key Laboratory of Magnetic Resonance and Atomic and Molecular Physics, National Center for Magnetic Resonance in Wuhan, Wuhan Institute of Physics and Mathematics, Innovation Academy for Precision Measurement Science and Technology, Chinese Academy of Sciences, Wuhan, Hubei 430071, China

<sup>e</sup> Interdisciplinary Institute of NMR and Molecular Sciences, School of Chemistry and Chemical Engineering, The State Key Laboratory of Refractories and Metallurgy, Wuhan University of Science and Technology, Wuhan 430081, China

<sup>f</sup> University of Chinese Academy of Sciences, Beijing 100049, China

## ARTICLE INFO

### Keywords:

Adsorption

Diffusion

Molecular sieves

PFG NMR

$^{129}\text{Xe}$  NMR

## ABSTRACT

Molecular sieves possess unique properties and have emerged as the predominant catalysts with shape selectivity in the petrochemical industry because of their well-defined pore architectures. However, the existence of a constrained pore surroundings of molecular sieves can limit intracrystalline diffusion, leading to underutilization of the active volume of the molecular sieve or rapid catalysts deactivation during catalytic processes. Moreover, the mechanism of adsorption and diffusion of molecules inside molecular sieves is crucial for the optimization and advancement of catalysts in heterogeneous catalysis. Due to the complexity of the diffusion process in molecular sieve materials, it is very necessary to develop characterization methods that are more sensitive and informative for studying the adsorption and diffusion of guests inside pores. Advancements in characterization techniques and theoretical calculations have led to a more profound comprehension of the adsorption and diffusion properties of molecular sieves at the microscopic scale. This article mainly summarizes the research progress of molecular adsorption and diffusion in molecular sieve materials using advanced  $^{129}\text{Xe}$  NMR, hyperpolarized (HP)  $^{129}\text{Xe}$  NMR, and pulsed-field gradient (PFG) NMR techniques in recent years and focuses on the principles of these techniques and applicability of the relationship of adsorption-diffusion using these techniques within several molecular sieve systems. Moreover, the effects of the topology and pore connectivity of molecular sieves on the adsorption and diffusion of guest molecules as well as the effects of intracrystalline diffusion on catalytic reactions are discussed.

## 1. Introduction

Molecular sieves, a class of porous solid materials, are widely used in adsorption, separation, catalysis, and especially in petrochemical industry, due to their sieving and confining effects. They can be divided into aluminosilicate zeolite and silicoaluminophosphate (SAPO) molecular sieve based on their elemental composition [1,2]. As classic solid acid catalysts, molecular sieves with high specific surface area, uniform pore, adjustable acidity and remarkable hydrothermal stability, are

commonly utilized in important chemical industrial processes including fluid catalytic cracking (FCC), methanol-to-olefins (MTO), hydrocracking and so on [1,3,4]. For example, the MTO reaction benefits significantly from the excellent shape selectivity of the SAPO-34 molecular sieve characterized by chabazite (CHA) topology. The faujasite (FAU) topology of Y zeolite makes it a crucial catalyst for the FCC process. On the other hand, ZSM-5 zeolite with MFI structure is extensively employed in methanol-to-gasoline (MTG) and methanol-to-propene (MTP) reactions due to its special pore structure. The unique catalytic

\* Corresponding authors at: National Engineering Research Center of Lower-Carbon Catalysis Technology, Dalian Institute of Chemical Physics, Chinese Academy of Sciences, Dalian 116023, China.

E-mail addresses: [zhenganm@wipm.ac.cn](mailto:zhenganm@wipm.ac.cn) (A. Zheng), [xushutao@dicp.ac.cn](mailto:xushutao@dicp.ac.cn) (S. Xu).

<https://doi.org/10.1016/j.jmro.2024.100180>

Available online 26 November 2024

2666-4410/© 2024 The Author(s). Published by Elsevier Inc. This is an open access article under the CC BY-NC license (<http://creativecommons.org/licenses/by-nc/4.0/>).

properties of mordenite (MOR) zeolite are responsible for its employment as a catalyst in the carbonylation of dimethyl ether (DME). In these heterogeneous catalytic processes, the pores of molecular sieves are not only the place of catalytic reactions but also an important channel for the adsorption and mass transport of reactants and products. Due to the pore dimension of less than 2 nm, adsorption and mass transport behaviors of molecules inside confined pores of microporous molecular sieves are closely related to pore structure, which also is a significant factor affecting its catalytic and separation application. Adsorption and diffusion in molecular sieves have attracted considerable attention for several decades. A comprehensive study of mass transport process of molecules inside the confined environment of molecular sieves and its influence on the efficiency of catalytic reactions is essential for developing a thorough comprehension of catalytic reaction processes, product selectivity, and the optimization and development of new catalysts. From the microporous and mesoporous molecular sieves to hierarchical molecular sieves, a lot of diffusion studies of guests in confined space have been conducted and remarkable progress has been accomplished [5,6]. The importance of understanding the mass transport performance of the products inside confined pores of molecular sieve catalysts for regulating product distribution is also pointed out in previous studies [7, 8]. Therefore, a thorough investigation of the adsorption and mass transfer process at the microscopic scale is crucial for understanding the separation or catalytic reaction mechanism.

The complexity and diversity of the adsorption and mass transport behavior observed in the confined pores of molecular sieves are one of the major challenges for diffusion measurement. To deepen the understanding of the molecular mass transport mechanisms within microporous materials, the past decades have witnessed a rapid development of a variety of experimental methods for measuring diffusion coefficient of molecules in porous materials [9,10]. Depending on the length of the diffusion pathway experienced by the molecule inside porous material during the experiment, the method of diffusion measurement can be classified as macroscopic, mesoscopic and microscopic measurements [9]. Macroscopic measurements are suitable for assessing the overall diffusion behavior among ensembles of crystals rather than within a single crystal, as the diffusion paths in these measurements extend significantly beyond the boundaries of individual crystals. Mesoscopic measurements concentrate on specific crystals and are also typically used to evaluate overall diffusion characteristics of the crystals. In contrast, microscopic measurements are primarily employed to analyze the diffusion behavior of molecules within an individual crystal. Among the previously reported works, microscopic measurements were particularly emphasized owing to their high sensitivity to the pore structure, cation ion, and interactions between different components of nanoporous materials. The diffusion coefficient measured by the microscopic method can reflect the diffusion limitation imposed by the topology on the molecule adsorbed in molecular sieves. In addition, molecular dynamics simulations have also played a crucial role in diffusion research in recent years [11,12]. Most importantly, the diffusion coefficients measured by the microscopic method can be directly compared with those simulated by molecular dynamics simulations. By employing both microscopic measurement techniques and theoretical simulations, a comprehensive knowledge of the adsorption and diffusion kinetics of guest molecules adsorbed in porous materials would be achieved. Pulsed field gradient nuclear magnetic resonance (PFG NMR) technique, a microscopic measurement method, can offer the self-diffusion coefficient of guest molecules, which reflects the average mass transfer information of the guest molecule within the crystal [6]. Additionally,  $^{129}\text{Xe}$  NMR and laser-hyperpolarized (HP)  $^{129}\text{Xe}$  NMR techniques exhibit high sensitivity towards the pore structure, as well as the position and distribution of guest molecules adsorbed in molecular sieves [13,14]. Taking advantage of PFG NMR,  $^{129}\text{Xe}$  NMR and HP  $^{129}\text{Xe}$  NMR approach, a series of studies to monitor the adsorption and mass transport behavior of guests inside the molecular sieve materials, by observing adsorption site, diffusion rate, and the interactions between

molecular and pores, were conducted [15–17]. In this paper, the recent research progress of PFG NMR,  $^{129}\text{Xe}$  NMR and HP  $^{129}\text{Xe}$  NMR for studying the adsorption and mass transfer processes of guest molecules adsorbed in molecular sieves are reviewed. Mass transfer of molecules within different topologies of molecular sieves is introduced. Additionally, the impacts of pore distribution on diffusion and selective adsorption, are also discussed. Finally, the impact of molecular sieve adsorption and diffusion mechanisms on catalytic reactions is explored. The combination of  $^{129}\text{Xe}$  NMR, HP  $^{129}\text{Xe}$  NMR and PFG NMR techniques can provide more comprehensive molecular dynamics information and reveal the complex relationship of adsorption-diffusion within molecular sieve materials.

## 2. NMR methods

Since 1946, Bloch [18] and Purcell [19] discovered  $^1\text{H}$  NMR in liquid water and solid paraffin, respectively, the NMR has become an indispensable and important tool in the disciplines of chemistry, physics, medicine, geology and biology. Typically, solid-state nuclear magnetic resonance (ssNMR) spectroscopy can offer detailed insights into the chemical structure at the atomic level due to its non-destructive and sensitivity to short-range interactions, which is widely applied in the study of molecular sieves catalyst, especially in the areas of capturing intermediates in catalytic reactions [20], probing pore structures [13], and analyzing host-guest interaction [5].

### 2.1. $^{129}\text{Xe}$ NMR

Xenon (Xe) is a noble gas and consists of nine stable isotopes. Of these isotopes,  $^{129}\text{Xe}$  and  $^{131}\text{Xe}$  both can be detected by NMR. However, compared with the isotope  $^{131}\text{Xe}$  ( $I = 3/2$ , natural abundance of 21.18 %),  $^{129}\text{Xe}$  ( $I = 1/2$ , natural abundance of 26.44 %) has higher NMR sensitivity and more simple spectra [21]. Xenon atoms demonstrate a high sensitivity to their surrounding chemical environment, which is attributed to their large and easily polarizable electron cloud. Any small alteration in the chemical environment can result in a change of NMR chemical shift. Compared to  $^1\text{H}$  and  $^{13}\text{C}$  NMR,  $^{129}\text{Xe}$  NMR exhibits a broader range of chemical shifts up to 7000 ppm for the xenon compounds, and provides more detailed spectral information. And the chemical shift range of  $^{129}\text{Xe}$  NMR for xenon adsorption in confined pores is often around 300 ppm [13,22]. These unique properties make  $^{129}\text{Xe}$  an ideal probe atom for studying structure, environment and connectivity of pores in molecular sieve materials. Since Brun et al. first reported the detection of  $^{129}\text{Xe}$  signals by NMR in 1954 [23],  $^{129}\text{Xe}$  NMR has gradually become a powerful characterization method for pore systems and has been widely used in several research fields including molecular sieves, polymers, liquid crystals, and metal-organic frameworks (MOFs) [13,14].

Fraissard et al. applied  $^{129}\text{Xe}$  NMR in the 1980s to study the pore structure of molecular sieve materials [24,25]. The signal for xenon atoms corresponding to adsorbed xenon will be observed in the  $^{129}\text{Xe}$  NMR spectrum when they interact with the pore surfaces or strong adsorption sites within the pores. Small changes in pore dimensions, connectivity between pores, pore type and the composition of the molecular sieve, would lead to the deformation of the electron cloud of xenon atom. These changes are then reflected in variations in chemical shift of  $^{129}\text{Xe}$  NMR.

In the  $^{129}\text{Xe}$  NMR spectra,  $^{129}\text{Xe}$  chemical shift of xenon absorbed in pores is expressed as the result of superposition of a variety of interactions proposed by Fraissard et al. [24]:

$$\delta = \delta_{\text{ref}} + \delta_s + \delta_{\text{Xe-Xe}} + \delta_{\text{SAS}} + \delta_E + \delta_M \quad (1)$$

where  $\delta_{\text{ref}}$  is assigned to 0 ppm, which represents the chemical shift of xenon gas at zero pressure.  $\delta_s$  reflects the interaction between xenon atoms and pore walls, which is usually associated with pore size and

pore shape.  $\delta_{\text{Xe-Xe}}$  describes the interaction between xenon atoms adsorbed in the pore and is proportional to the density of xenon atoms.  $\delta_{\text{SAS}}$  refers to the interaction between xenon and a strong adsorption site.  $\delta_{\text{E}}$  and  $\delta_{\text{M}}$  are affected by the existence of an electrostatic field and magnetic field, respectively.

Several articles have reviewed the studies on the pore structure, chemical composition, effect of cations, distribution of adsorption site, and location of carbon deposition of molecular sieve catalysts by  $^{129}\text{Xe}$  NMR at various temperatures or pressures [13,14,22].

## 2.2. Hyperpolarized (HP) $^{129}\text{Xe}$ NMR

The improvement of the sensitivity of NMR has always been the focus of NMR research. The use of  $^{129}\text{Xe}$  NMR is limited when xenon adsorbed in porous materials at low concentrations due to its low sensitivity. By using laser HP xenon produced by optical pumping, the sensitivity of  $^{129}\text{Xe}$  NMR can be improved by about 4–5 orders of magnitude. And due to the continuous flow of HP  $^{129}\text{Xe}$  into the probe, the NMR measurements are not significantly affected by the relaxation time of  $^{129}\text{Xe}$ , resulting in a considerable reduction in acquisition time [26,27]. Moreover, the introduction of in-situ continuous flow and magic angle spinning (MAS) techniques [27,28] has greatly promoted the development of  $^{129}\text{Xe}$  NMR techniques in porous materials [28,29].

In the 1980s, Happer et al. discovered the NMR spectra of polarized  $^{129}\text{Xe}$  [30]. After that, Pines et al. [31] applied optical pumping to  $^{129}\text{Xe}$  NMR. Zeng [32] acquired a  $^{129}\text{Xe}$  NMR signal by spin exchange of cesium and the xenon signal is greatly enhanced. The basic principle and application of HP  $^{129}\text{Xe}$  NMR have been reviewed in many literatures [14].

HP  $^{129}\text{Xe}$  NMR is successfully achieved by spin-exchange optical pumping (SEOP) [33]. In the SEOP process, the polarization of the electronic spin of the alkali-metal is transferred to the  $^{129}\text{Xe}$  nucleus by hyperfine interactions, in which xenon is contact with rubidium gas in a mixed gas containing xenon, nitrogen and helium. Fig. 1 illustrates the basic principle of the production of hyperpolarized xenon by the SEOP process [34], which mainly includes the optical pumping of the electronic spins of the alkali metal atoms (Fig. 1a) and the polarization of xenon nuclei via collision and spin-exchange (Fig. 1b). In optical pumping, a polarized non-Boltzmann population of rubidium atoms is created by irradiating gaseous rubidium atoms with a circularly polarized laser at 794.4 nm in a magnetic field, corresponding to the D1 line of Rubidium (Rb). The angular momentum of alkali atom was transferred to the inert gas nucleus through hyperfine interaction during the spin-exchange process after the alkali metal atoms are polarized, resulting in a highly hyperpolarized  $^{129}\text{Xe}$ .

HP  $^{129}\text{Xe}$  NMR has proven to be crucial for analyzing the structural

and dynamic properties of pores in porous materials. Even at low xenon concentration, the sensitivity of HP  $^{129}\text{Xe}$  NMR can be enhanced by 3–5 orders of magnitude, which is very effective for the detection of a small number of samples and the observation of the non-equilibrium process. Additionally, the variable temperature HP  $^{129}\text{Xe}$  NMR technique can sensitively detect the pore connectivity of porous materials and distinguish the hierarchical structure in molecular sieve materials, which provides a guidance for the preparation, characterization and application of the hierarchical molecular sieve materials.

## 2.3. Two-dimensional (2D) exchange spectroscopy (EXSY)

For molecular sieves with multiple pores on different length scales, the characterization of the connectivity of different channels is also crucial. Jeener et al. [35] developed two-dimensional (2D) exchange spectroscopy (EXSY), an effective technique for the research of exchange process. By merging chemical sensitivity features of xenon with two-dimensional exchange spectra, 2D  $^{129}\text{Xe}$  EXSY NMR emerges as a potential tool for clarifying the structural properties of molecular sieves [13,36]. 2D  $^{129}\text{Xe}$  EXSY NMR can be used to investigate the exchange process of xenon atoms adsorbed inside molecular sieve materials. This method can offer comprehensive information on the connectivity between pores and the distribution of different adsorption sites in porous materials. The pulse sequence of 2D EXSY NMR is shown in Fig. 2. In 2D EXSY NMR experiments, by changing the mixing time ( $\tau_{\text{mix}}$ ), the detection of the dynamic exchange between different sites through NMR can be achieved. In the 2D  $^{129}\text{Xe}$  EXSY NMR spectrum, the cross-peaks at off-diagonal positions represent the occurrence of the xenon exchange process in different sites within the mixing time. This feature makes the 2D  $^{129}\text{Xe}$  EXSY NMR technique particularly interesting for the research of molecular sieve materials with a hierarchical pore structure. The connectivity between the pores of the two crystalline phases can be determined by changing the mixing time in the 2D  $^{129}\text{Xe}$  EXSY NMR spectrum. Additionally, 2D  $^{129}\text{Xe}$  EXSY NMR also can reveal the exchange dynamics of xenon between different adsorbed sites within pores of molecular sieve.

## 2.4. Pulsed field gradient (PFG) NMR

PFG NMR, a non-destructive technique, can monitor the movement of guest molecules within porous materials by using a pulsed field gradient to mark the spatial position of the observed nuclear spins, allowing for the assessment of the diffusion behavior of the guest molecules [6]. PFG NMR provides the average mass transfer information of guest molecules within the crystal, with spatial and temporal scales on the order of micrometers and milliseconds, respectively. Currently, this approach is extensively utilized to investigate the mass transport behavior of molecules in porous materials.

In the 1970s, Pfeifer and Kärger et al. [9] conducted a study on the molecular motion in porous materials by applying PFG NMR. With the development of NMR pulse sequences, pulsed gradient spin echo (PGSE), pulsed gradient stimulated echo (PGSTE) and pulsed gradient stimulated echo using bipolar gradients (also known as a 13-interval sequence) have been developed [37,38]. With the expansion of application systems,  $^1\text{H}$  PFG NMR,  $^{13}\text{C}$  PFG NMR,  $^{19}\text{F}$  PFG NMR,  $^{129}\text{Xe}$  PFG NMR, and so on, have also been successfully applied in mass transfer research [39–41]. Moreover, recent advancements have led to the development of magic angle spinning (MAS) PFG NMR with higher spectral resolution. This advanced NMR technique is employed to differentiate between signals from various hydrocarbons in mixtures and is extensively applied in the diffusion study of hydrocarbon mixtures adsorbed in porous materials [42,43].

Taking the typical PGSE sequence as an example, the measurement principle of the self-diffusion coefficient using PFG NMR is illustrated in Fig. 3 [37]. Under an external magnetic field with a strength of  $B_0$  in the z-direction, the Larmor frequency ( $\omega$ ) of nuclear spin is expressed as:

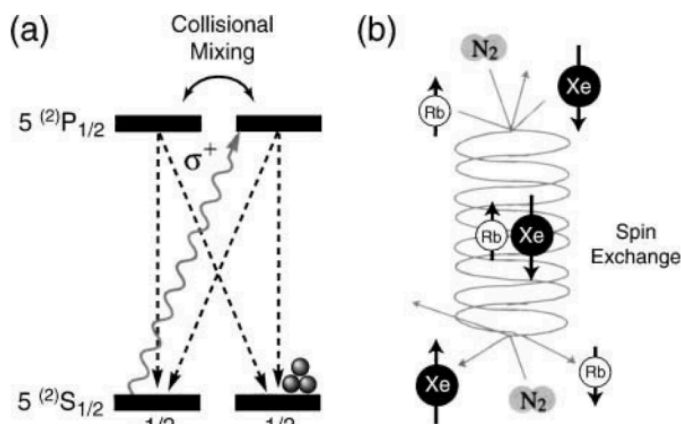


Fig. 1. Schematic diagram of (a) the optical-pumping process and (b) the spin-exchange process of alkali-metal [34].

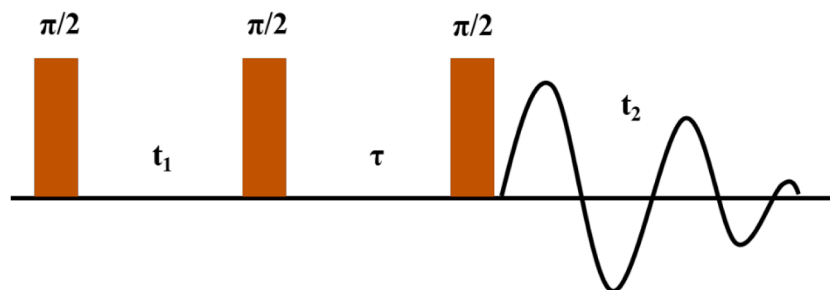


Fig. 2. General EXSY pulse sequence [35].

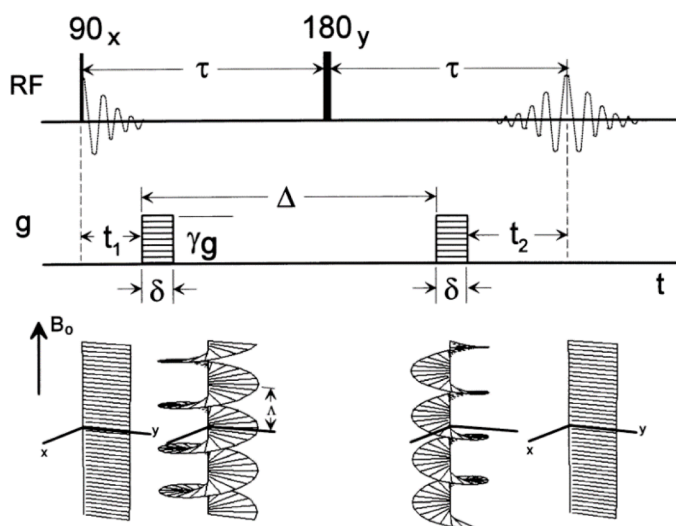


Fig. 3. Diagram of pulsed gradient spin echo sequence [37].

$$\omega = \gamma B_0 \quad (2)$$

$\gamma$  denotes the gyromagnetic ratio of the observed nucleus. If an additional field gradient is introduced along the direction of magnetic field (Z direction) over a short time interval,  $z$  is the  $z$ -axis coordinate,  $g$  is the field gradient intensity, and the total magnetic field strength varying with position becomes:

$$B = B_0 + gz \quad (3)$$

In this way, the Larmor frequency of the nuclear spins as a function of the  $z$ -axis coordinate:

$$\omega(z) = \gamma B_0 + \gamma gz \quad (4)$$

The spatial positions of different nuclear spins therefore are marked by a pulsed field gradient and the phase of nuclear spins are obtained. The field gradient pulses have identical magnitude and duration in the spin-echo sequence. The first field gradient pulse is applied after a  $90^\circ$  radio frequency (RF) pulse. The de-phasing of the vectors of transverse magnetization takes place and the phase of the nucleus is labeled by the field gradient. If the position of the individual molecule remains unchanged during the time interval between the two field gradient pulses, the phase of the spins is re-focused and the transverse magnetization vector is completely restored after applying the  $180^\circ$  RF pulse, followed by the second field gradient pulse. The de-phasing caused by the initial field gradient pulse is fully compensated by the subsequent field gradient pulse, resulting in a net phase of zero. During the interval between the two field gradient pulses, if the position of the individual molecule changes, the incomplete re-focusing of the spins and a phase difference ( $\Delta\phi$ ) are obtained. Thus, the difference in the position of individual spins can be acquired because the  $\Delta\phi$  can be detected by NMR.

The attenuation of spin echo caused by molecular diffusion, is expressed as the Stejskal–Tanner-Equation:

$$\Psi(g, t) = \frac{I(g)}{I(0)} = \exp(-\gamma^2 \delta^2 g^2 D t) = \exp\left(-\gamma^2 \delta^2 g^2 D \left(\Delta - \frac{\delta}{3}\right)\right) \quad (5)$$

where  $I(0)$  and  $I(g)$  are the intensity of NMR signal when the field gradient intensity is zero and  $g$ , respectively, and  $\delta$  represents the effective gradient pulse duration.  $\Delta$  denotes the time interval between the two field gradient pulses.  $D$  is the self-diffusion coefficient. A series of attenuation signals are obtained by linearly increasing  $g$  with constant  $\delta$  and  $\Delta$  in PFG NMR experiments. In general, the values of  $\delta$  and  $\Delta$  range from 0.1 to 10 ms and 1 to 1000 ms, respectively.

In PFG NMR measurements, it is essential to choose suitable pulse sequences according to the characteristics of different systems for the accurate measurement of diffusion coefficient. In PGSE sequence, the maximum observation time of NMR signal is limited by the transverse relaxation time,  $T_2$ , which is usually on the order of a few milliseconds [44]. In PGSTE sequence, the observation time can be significantly extended. In this case, the maximum observation time is governed by the longitudinal relaxation time,  $T_1$ , which can reach several seconds [45]. Therefore, the PGSE sequence is generally preferred when  $T_1$  equals  $T_2$  in the sample. When  $T_1$  is significantly greater than  $T_2$ , the PGSTE sequence is often employed. For porous materials, the internal magnetic susceptibility is different due to the inhomogeneity of structure, which further leads to different magnetic field gradients induced by the external magnetic field. Cot et al. [38] developed a pulsed gradient stimulated echo using bipolar gradients (or 13-interval). Based on PGSTE, the original unipolar gradient pulse is divided into two gradient pulses with positive polarity and negative polarity by  $180^\circ$  RF pulse, which greatly improves the accuracy of diffusion measurement.

The PFG NMR technique provides significant advantages for studying molecular mass transport and dynamics within molecular sieves. However, it still faces several limitations, particularly in the measurement of slow diffusion systems. In the measurement of such systems, the minimal molecular displacement results in weak signal attenuation caused by diffusion. The weak attenuation makes it difficult to distinguish the signal difference in the measurement of diffusion coefficient, especially in a low signal-to-noise ratio (SNR), resulting in increased errors in the diffusion coefficient measurements. Thus, stronger magnetic field gradients are typically required to achieve sufficient signal attenuation. Additionally, slow diffusion systems often exhibit shorter  $T_2$ , causing rapid signal decay, which complicates the detection of signals. Accurate measurement of diffusion coefficients in these cases requires well-designed pulse sequences that minimize the effects of  $T_2$  relaxation, and supported by high-performance hardware. Moreover, the reaction system catalyzed by molecular sieve typically involves complex multi-component, multiphase environments, extreme reaction conditions, and dynamic chemical environments. These factors make the measurement of diffusion coefficients using PFG NMR more challenging in such systems. This requires special optimization of experimental design, signal analysis, and equipment performance to obtain accurate diffusion coefficient measurements.



Currently, numerous studies have been conducted to explore the mass transfer behavior of guest molecules absorbed in porous materials using PFG NMR, aiming to clarify the catalysts performance and catalytic reaction mechanism from the perspective of the mass transfer mechanism. Kärger group has made many important achievements in the diffusion mechanism of porous materials by using the PFG NMR technique [5,42,46]. Furthermore, the observation of the interaction between guest molecules and the molecular sieve framework at the atomic scale is also a great challenge by experimental methods. Due to adjustable and more targeted parameters in simulation, molecular dynamics simulations exhibit an advantage in exploring the host-guest interactions [47,48]. A comprehensive understanding of adsorption and mass transfer mechanisms in molecular sieves is achieved by using PFG NMR,  $^{129}\text{Xe}$  NMR, and molecular dynamics simulations.

### 3. Recent advances in NMR for adsorption and mass transport in molecular sieves

#### 3.1. Adsorption distribution in molecular sieves

The adsorption process is a prerequisite for diffusion, and the essence of diffusion is the migration process of molecules at different adsorption sites. Previous researches reveal that different adsorption sites of guest molecules in molecular sieves will affect their diffusion behavior [49, 50]. Using xenon as a probe atom,  $^{129}\text{Xe}$  NMR can be employed to investigate the distribution of guest molecules and the dominant adsorption sites inside pores or crystals of molecular sieve. A thorough understanding of the distribution of adsorption sites in catalysts can offer a theoretical foundation for the development and synthesis of high-performance industrial catalysts/adsorbents by understanding the adsorption-diffusion-reaction relationship at the atomic level.

Using  $^{129}\text{Xe}$  NMR,  $^{129}\text{Xe}$  MAS NMR and 2D EXSY NMR, Gao et al. [49] revealed the existence of  $\text{Xe}_n$  ( $n = 2-5$ ) clusters with different sizes in a single SAPO-34 crystal at the microscale. These  $\text{Xe}_n$  clusters are distributed from the outer layers to the core of the crystal, becoming smaller in size.  $^{129}\text{Xe}$  PFG NMR experiment exhibits a strong correlation between the self-diffusion coefficient of the adsorbed xenon and xenon concentration in SAPO-34. The  $\text{Xe}_n$  clusters with high xenon concentration located on the outer layers of crystal have higher diffusion coefficients. Furthermore, the correlation between the adsorption feature and diffusion behavior of xenon in the SAPO-34 molecule sieve from the nano-scale to the micro-scale is established. The non-uniform distribution of  $\text{Xe}_n$  clusters in crystal leads to the difference of inter-cavity diffusion in SAPO-34 crystal, which causes the gradient distribution of adsorption and diffusion in molecular sieves.

Moreover, metal-ion modification, as a simple and efficient technique, is often employed to adjust catalytic reaction or adsorption performance in the design and modification of molecular sieve catalysts or adsorbents. The introduction of metal ions can not only modulate the strength and density of the acid site of molecular sieves but also modify the pore structure and affects the adsorption property and mass transfer behavior. Samant et al. [51] reported the existence of  $\text{Xe}_n$  clusters, containing different xenon atoms, within the  $\alpha$  cage of NaA zeolite. In  $^{129}\text{Xe}$  NMR spectra, five adsorption peaks of xenon with distinct chemical shifts value were presented. The adsorbed  $^{129}\text{Xe}$  chemical shifts related to xenon-xenon interaction means that these five signals correspond to different xenon atoms in  $\alpha$  cages, namely  $\text{Xe}_1$ ,  $\text{Xe}_2$ ,  $\text{Xe}_3$ ,  $\text{Xe}_4$  and  $\text{Xe}_5$ , respectively. These resolved adsorption signals observed in the  $^{129}\text{Xe}$  NMR spectra also indicate that the diffusion process of xenon atoms between adjacent cages is severely limited, and xenon atoms cannot exchange rapidly in adjacent cages. Furthermore, Larsen et al. [52], employed 2D  $^{129}\text{Xe}$  EXSY NMR to explore the inter-cages movement of xenon atoms in NaA zeolite. The energy required for diffusion between inter-cages was calculated to be 60 KJ/mol. However, in CaA zeolite, due to the larger eight-membered ring window modified by the  $\text{Ca}^{2+}$  ion compared to that of the  $\text{Na}^+$  ion, the rapid exchange between

$\text{Xe}_n$  clusters leads to one adsorbed xenon signal observed in  $^{129}\text{Xe}$  NMR spectrum of CaA zeolite [53].

The discussion on heterogeneity consistently emerges as a fundamental consideration in the research of catalyst performance. The manifestation of heterogeneity at the microscopic scale, be it at the micron or nanometer dimension, is worthy of attention. Particularly at the nanoscale, the essence of such heterogeneity can be ascribed to the disparity between the internal structure and surface of the catalyst. These variances at the microscopic level are ultimately reflected in the macroscopic performance of the catalyst. This scale of heterogeneity has a considerable influence on the catalyst's activity and selectivity and is also essential for the exploration and comprehension of catalyst properties. Besides the nonuniform adsorption in the crystal of SAPO-34 molecule sieves on a micro-scale, Gao et al. [50] also revealed the nonuniform adsorption on a nano-scale for DNL-6 molecule sieves by variable pressure  $^{129}\text{Xe}$  NMR and  $^{129}\text{Xe}$  PFG NMR experiments (Fig. 4). Unlike the SAPO-34 molecular sieve with a uniform cage environment of CHA, the DNL-6 molecular sieve consists of a *lta* cage and a double eight-membered ring (D8R) (Fig. 4a). As shown in Fig. 4b and d, the loading-dependent  $^{129}\text{Xe}$  NMR experiments and theoretical calculations show that there are three different xenon adsorption sites inside RHO structure of DNL-6 molecular sieves. The D8R is the preferred adsorption site for xenon, followed by the edge of the *lta* cage, and the center of the *lta* cage is the most difficult to be adsorbed.  $^{129}\text{Xe}$  PFG NMR diffusion studies show that the D8R, as the most preferred xenon adsorption site in the RHO structure, contributes to the increase of the mass transfer resistance for diffusion of xenon. At high xenon concentrations, the jump between inter-cages of xenon could be inhibited due to the preferential occupation of some xenon in D8R, which results in the decrease of self-diffusion coefficient of xenon within DNL-6 molecular sieve (Fig. 4c).

#### 3.2. Selective adsorption

For molecular sieve materials with structures consisting of different channel systems, guest molecules adsorbed in molecular sieve exhibit obvious adsorption selectivity in different pores. MOR zeolite is an important catalyst for MTO and DME carbonylation processes. The topology of MOR zeolite consists of straight ellipsoidal twelve-membered ring (12 MR) main channels and eight-membered ring (8 MR) side pockets. Gong et al. [54] investigated the adsorption selectivity of methanol and water guest molecules on various channels of MOR zeolite using *in-situ*  $^{129}\text{Xe}$  NMR and co-adsorption experiments. The results revealed notable differences in the adsorption behaviors of methanol and water on the MOR zeolite. Methanol exhibits a preference for adsorption on 12 MR main channels, and water tends to adsorb at the junctions between the main channels and side pockets. This understanding is crucial for explaining the variations in catalytic efficiency observed with MOR zeolite.

The adsorption selectivity of guest molecules in different pores of molecular sieves directly affects the catalytic performance in catalysis. In the study of the Fischer-Tropsch synthesis (FTS), Jiao et al. [55] studied the preferred adsorption sites for methanol and ketene intermediates on the MOR zeolite, respectively, using the xenon atom as a probe. As shown in Fig. 5,  $^{129}\text{Xe}$  NMR experiments exhibit that ketene is preferentially adsorbed in the 8 MR channel, while methanol is preferentially adsorbed in 12 MR channel. Combined with the catalytic reaction results and acidity characterization, it is proved that ketene may be an important intermediate for syngas conversion over the ZnCrOx-MOR catalyst.

#### 3.3. Dynamic behavior in different adsorption sites

The dynamic exchange behavior exhibited by different adsorption sites within molecular sieves is crucial for the efficiency and selectivity of the adsorption process. This phenomenon is intrinsically related to the

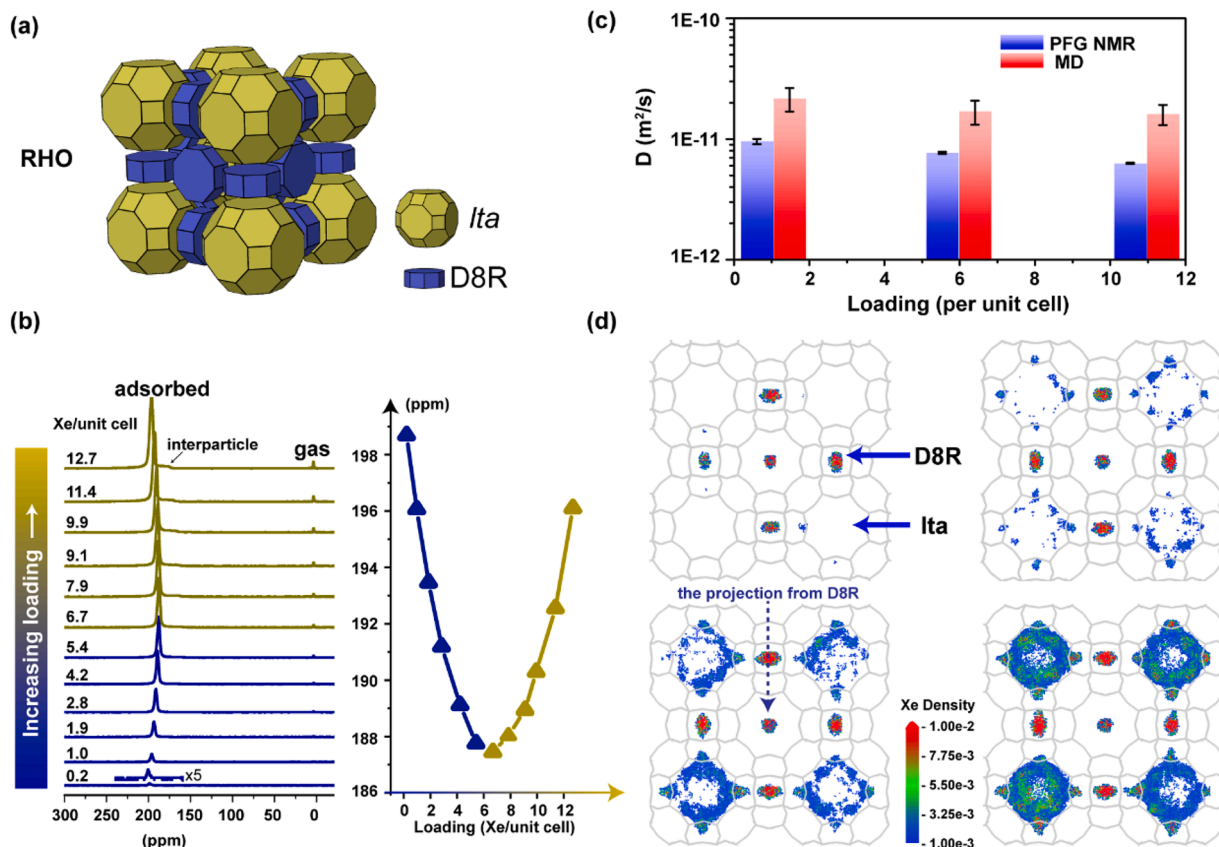


**Fig. 4.** (a) 3D filling of RHO structure. (b)  $^{129}\text{Xe}$  NMR spectra and corresponding chemical shift values of xenon in the adsorbed state within DNL-6 molecule sieve at variable concentration at 298 K. (c) The PFG NMR and MD self-diffusion coefficient of xenon in DNL-6 molecule sieve at 298 K, as a function of loading (d) Density maps of xenon adsorbed in RHO at different xenon loading [50].

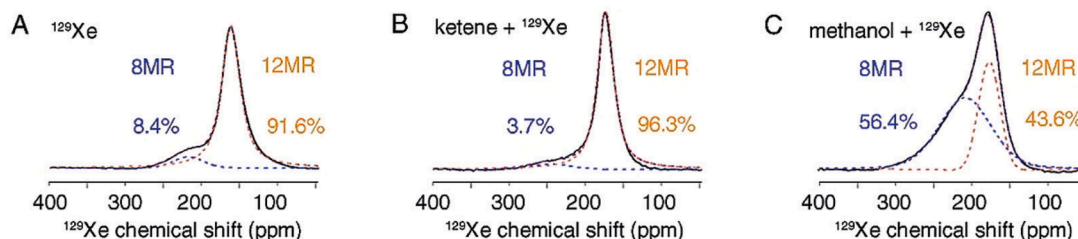


**Fig. 5.**  $^{129}\text{Xe}$  NMR spectra of ketene and methanol adsorbed on MOR, respectively [55].

microscopic interaction between adsorbed species and pore surfaces of molecular sieves. By elucidating the microscopic processes and the factors influencing the dynamic exchange between different adsorption sites, a deeper comprehension of the dynamic exchange mechanisms of guest molecules inside molecular sieves can be achieved. Furthermore, investigations into the dynamic behaviors of these adsorption sites also offer insights into the diffusion process of adsorbates within molecular sieves. Such research holds significant theoretical and practical implications for the exploration and production of high-efficiency molecular sieve materials, as well as for promotion of efficient separation and catalysis in industrial applications.

In the research by Qin et al. [56], a series of cavity-type mesoporous FAU zeolites that were created through unbiased leaching with  $\text{NH}_4\text{F}$  were studied by using HP  $^{129}\text{Xe}$  NMR and 2D EXSY NMR techniques. It was found that the smaller sodalite (SOD) cages of FAU zeolites were opened and gradually merged with supercages to form mesopores of 2 to 3 nm. Furthermore, the dynamic process of xenon atoms in different cages was analyzed. As shown in Fig. 6, diffusion paths of xenon atoms

in SOD cages and supercage were presented. Xenon atoms first enter the opened SOD cage from the gas phase and rapidly exchange between the SOD cage and supercage. Subsequently, xenon moves from the gas phase into the supercage and xenon atoms from the supercage diffuse into the gas phase. Finally, xenon within the SOD cage also diffuses into the gas phase. This work enhances the understanding of the evolution of cages for FAU zeolites and the relationship between pore structure and diffusion properties.

The different xenon exchange behaviors within two separate pore systems of MCM-22 zeolite was observed by Deng et al. using 2D  $^{129}\text{Xe}$  EXSY NMR at high xenon pressure (higher than 6 atm) [57]. As shown in Fig. 7, at lower temperatures of 170–122 K, the fast xenon exchange (less than 1 ms) between distinct adsorption regions within the same 12 MR supercage was observed. The xenon in the 12 MR supercage is exchanged with the xenon in the sinusoidal channel via the gaseous xenon in the interparticle space at high temperatures (280–350 K). This study offers important perspectives on the adsorption behavior in complex pore structures. Specifically, it highlights the significant impact of

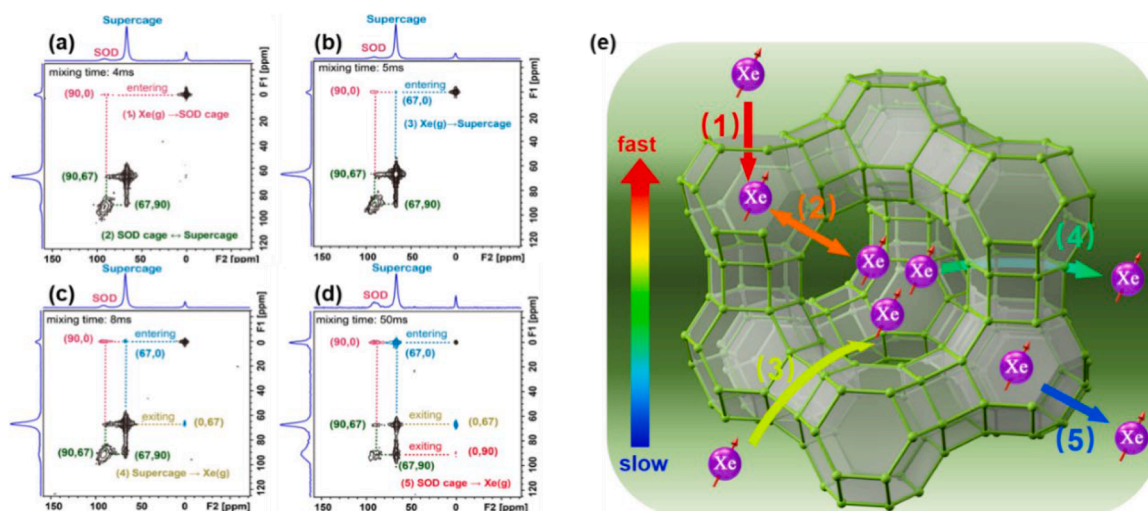


**Fig. 6.** 2D HP  $^{129}\text{Xe}$  EXSY NMR and diffusion pathways of xenon in FAU zeolite. (a) The gas phase xenon atom diffuses and adsorbs into the SOD cage and the xenon exchange between the SOD cage and the supercage. (b) Gaseous xenon diffuses and adsorbs into the supercage and (c) the xenon atoms adsorbed supercage diffuse to the gas phase. (d) The xenon atoms adsorbed SOD cage diffuse to the gas phase. (e) Graphical representation diffusion process of xenon in hierarchical FAU zeolite [56].

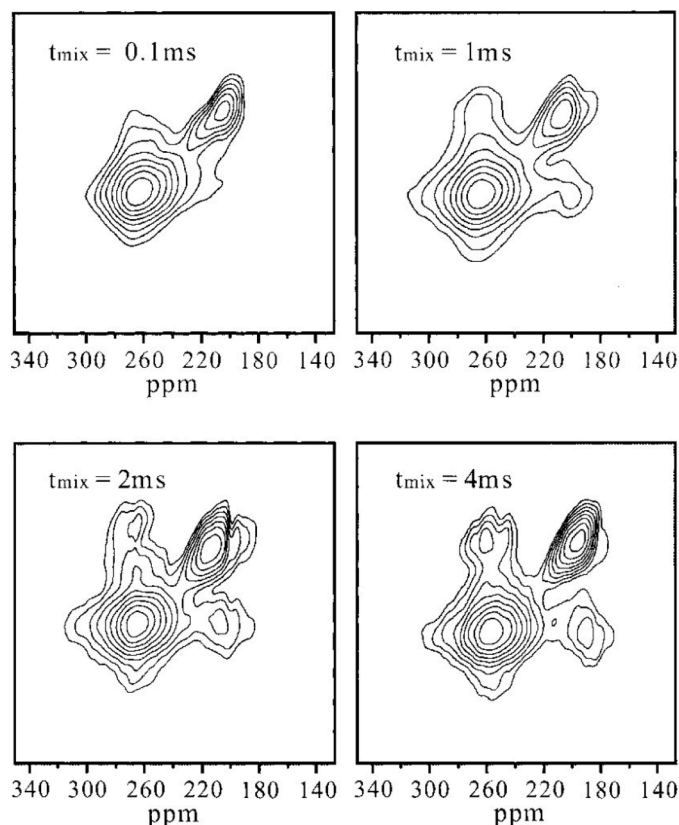


**Fig. 7.** 2D  $^{129}\text{Xe}$  EXSY NMR spectra for xenon inside MCM-22 zeolite as a function of mixing times at 145 K [57].

temperature on the xenon exchange dynamics within molecular sieves.

### 3.4. Diffusion in different topology

Molecular sieves are typically confined nanoreactors with a pore diameter of less than 2 nm. The adsorption properties and diffusion characteristics of molecules within the confined space of molecular sieves are quite different compared to those in bulk materials, including

unique phenomena like single-file diffusion [58] and window effects [59]. Previous research has demonstrated that the pore structure of molecular sieves, including the shape and dimensions of the pores, significantly influence the adsorption and mass transfer behavior of guest molecules [48,60,61].

The eight-membered ring and cavity structure molecular sieves have attracted considerable attention because of their excellent catalytic performance in MTO reactions and unique selectivity for olefin products. The mass transfer processes of alkanes (methane, ethane and propane) within cavity-type SAPO molecular sieves, specifically SAPO-35 featuring LEV topology, SAPO-34 with CHA topology, and DNL-6 characterized by RHO topology, were studied by Gao et al. [62] using PFG NMR technique and theoretical calculations (Fig. 8). The results show that as the cage size increases, the self-diffusion coefficients ( $D$ ) of alkanes increase, with the trend being  $D_{\text{SAPO-35}} < D_{\text{SAPO-34}} < D_{\text{DNL-6}}$ . Combined with theoretical calculations, the inter-cage hopping process of methane in an eight-membered ring and cavity structure molecular sieve was simulated, and the diffusion trajectory of methane was quantitatively analyzed. The diffusion-related parameters, specifically the frequency and length of jump, were determined. The reasons for the differences in alkane diffusion among the three kinds of cavity-type molecular sieves are given from a microscopic perspective. As shown in Fig. 8h, the inter-cage jump process of methane in the LEV structure has the lowest jump frequency (0.4/ns) and the shortest jump length (8 Å), which corresponds to the lowest diffusion coefficient. However, the inter-cage jump process of methane in RHO has a high jump frequency (2.8/ns) and the longest jump length (14.8 Å), showing the fastest diffusion behavior. Correlating cage structure and jump frequency, cage size and jump length, respectively, it is found that cage structure determines the energy barrier of the jump between adjacent cages and the jump frequency of molecules. The jump length depends on the distance between adjacent cages. Therefore, the diffusion mechanism controlled by cavity structure in an eight-membered ring and cavity-type molecular sieve is proposed.

ZSM-5 zeolite, widely used as shape-selective catalyst, has been extensively applied in heterogeneous catalytic processes, including MTO, alkylation, and aromatization. ZSM-5 zeolite, which features a MFI topology, has straight channel formed by ten-membered ring (10 MR) ( $5.3 \times 5.6$  Å) and sinusoidal channel formed by 10 MR ( $5.1 \times 5.5$  Å). The small difference in pore size significantly influences the diffusion behavior of guest molecules and the selectivity of products. The elucidation of the diffusion behaviors in two-channel systems can contribute



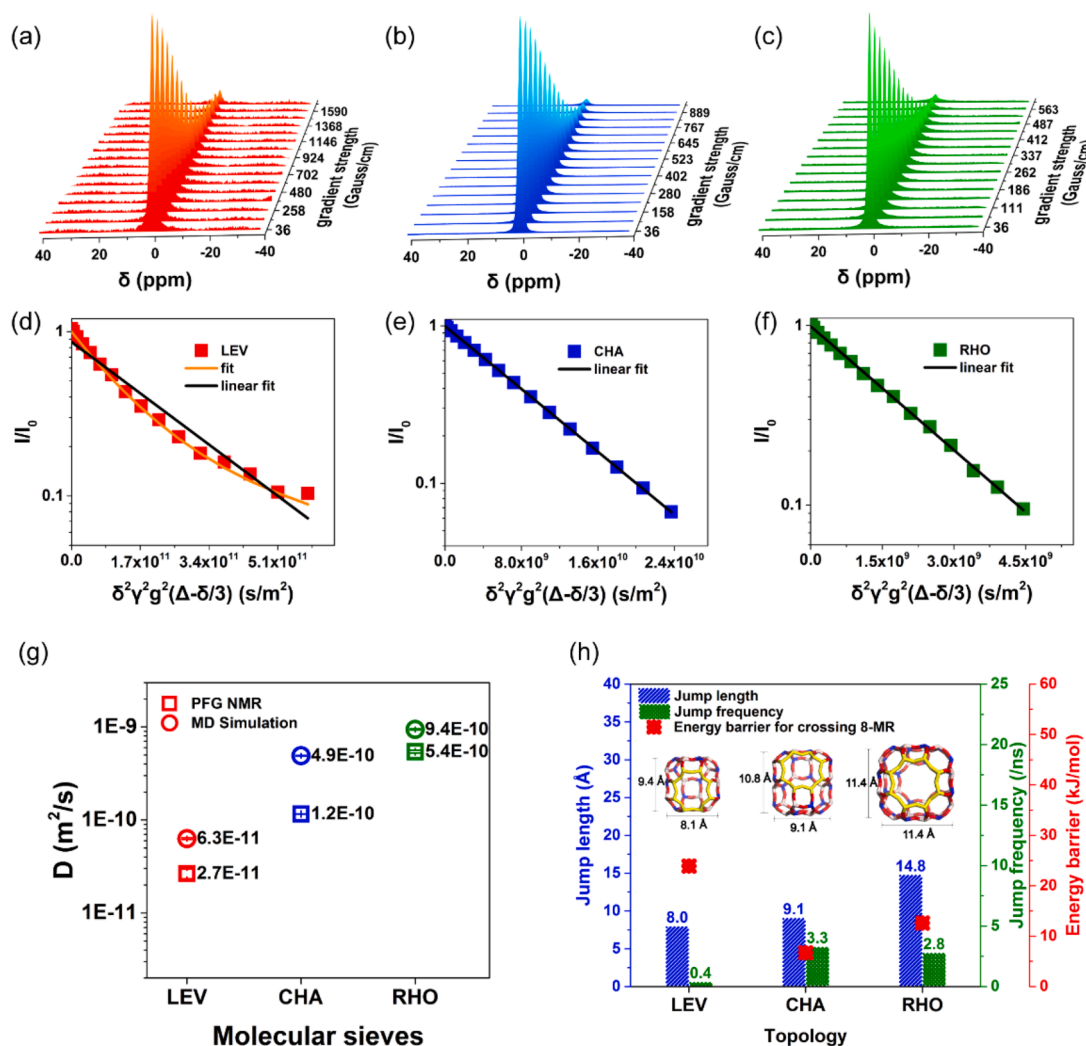


**Fig. 8.** (a–c) The decay of  $^1\text{H}$  PFG NMR signals measured at 298 K in LEV, CHA and RHO with a increased field gradient strength. (d–f) Corresponding attenuation of PFG NMR spin echo as a function of  $\delta^2 \gamma^2 g^2 (\Delta - \delta/3)$  for LEV, CHA and RHO. (g) The self-diffusion coefficients of methane in LEV, CHA and RHO, measured by PFG NMR and MD simulation, respectively. (h) The jump frequency, jump length and energy barrier associated with methane diffusion through 8-MR of LEV, CHA and RHO [62].

to more effectively clarifying product selectivity during catalytic reactions and guiding the development of catalysts with enhanced reaction performance.

The different intracrystalline diffusion behaviors of n-butane and isobutane within ZSM-5 zeolite were revealed by Zeng et al. using  $^1\text{H}$  PFG NMR [60]. In the ZSM-5 zeolite, isobutane predominantly diffuses through straight channels, whereas n-butane exhibits an equal probability of distribution between sinusoidal and straight channels. As depicted in Fig. 9, the diffusion coefficients of n-butane in two channels of the ZSM-5 zeolite were successfully distinguished by introducing the diffusion tensors in different directions. The diffusion coefficients of n-butane in sinusoidal channels were approximately  $10^{-10}$  m $^2$ /s, and that in straight channels were in the order of  $10^{-9}$  m $^2$ /s, indicating that the straight channels of ZSM-5 zeolite exhibit better transport ability. The variation in molecular diffusion behavior indicates the heterogeneity of pore channels, leading to anisotropic molecular diffusion.

### 3.5. Diffusion in hierarchical molecular sieves

Although the micropore of molecular sieve provides required confinement effect and excellent shape selectivity for catalytic reaction, the diffusion process of larger reactant or product molecules is severely limited, which results in a shorter catalyst lifespan and lower utilization

of the molecular sieve catalyst. The preparation and application of hierarchical molecular sieves have been widely developed in recent years [63,64]. Introducing mesopores and/or macropores into a microporous molecular sieve can tremendously enhance mass transport efficiency and has demonstrated remarkable catalytic performance in heterogeneous catalysis and other areas.

The enhancement of mass transfer is always the core for the design of hierarchical structures in hierarchical molecular sieves. Appropriate characterization tools for mass transfer are crucial for the optimization of mass transfer performance of materials. PFG NMR and  $^{129}\text{Xe}$  NMR, as characterization methods of diffusion studies at the microscopic level, have been extensively applied in various hierarchical molecular sieves. Kärger et al. [46] pioneered the use of PFG NMR to evaluate the diffusion properties of nano-sheet NaX zeolite with a hierarchical structure. Compared with pure microporous NaX zeolite, the diffusion of probe molecules is enhanced by an order of magnitude in nano-sheet NaX zeolite, which proves the improved mass transport attributed to the introduction of mesoporous and macroporous in microporous materials. Galarneau et al. [65] used PFG NMR to assess the pore connectivity of hierarchical zeolites. The diffusion results indicate that improved diffusion performance is attributed to interconnected micropores and mesopores.

Sun et al. [63] used probe molecule of methane to determine the



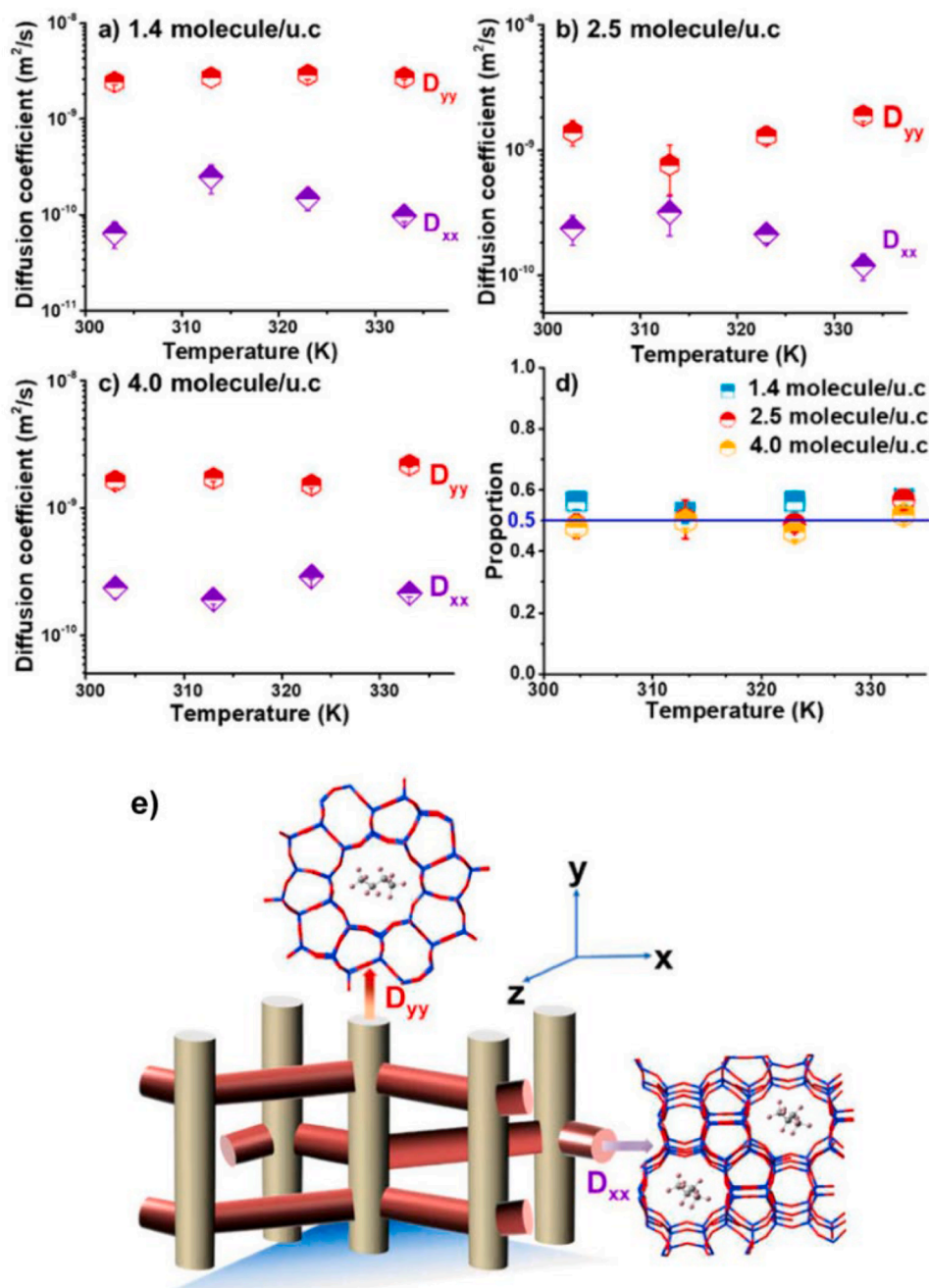


**Fig. 9.** (a–c) The self-diffusion coefficients of n-butane in straight and sinusoidal channel of ZSM-5 zeolite vary as the temperature ranges from 303 K to 333 K under different loading, respectively; (d) The probability of n-butane molecules in the straight channel at various temperatures; (e) Schematic illustration of n-butane diffusion through straight and sinusoidal channel of ZSM-5 zeolite [60].

self-diffusion coefficient of ZSM-5 zeolite with a well-organized macro-meso-microporous structure (OMMM) using  $^1\text{H}$  PFG NMR. Compared to the microporous ZSM-5, OMMM-ZSM-5 showed greatly improved mass transfer performance and the diffusion coefficient of methane in OMMM-ZSM-5 was an order of magnitude greater than in the microporous ZSM-5, which indicated that the introduction of mesopores and macropores in OMMM-ZSM-5 enhances methane diffusion.

Furthermore,  $^{129}\text{Xe}$  NMR and HP  $^{129}\text{Xe}$  NMR are also extremely sensitive techniques that can be utilized to uncover the pore connectivity in porous materials. Particularly, at low temperatures, the xenon exchange between distinct pores is seriously limited and two independent signals assigned to xenon absorbed in micropores and mesopores can be presented in  $^{129}\text{Xe}$  NMR spectra, respectively. Liu et al. [27]

employed HP  $^{129}\text{Xe}$  NMR and  $^{129}\text{Xe}$  2D EXSY NMR to evaluate the mass transfer performance of ZSM-5 zeolite-containing mesopores (denoted as Meso-ZSM-5). Two kinds of Xe signals adsorbed on micropores and mesopores were observed by variable temperature HP  $^{129}\text{Xe}$  NMR experiments (Fig. 10), respectively. Simultaneously, observations from 2D EXSY NMR demonstrate that even at extremely low temperatures, the rate of xenon exchange between micropores and mesopores of Meso-ZSM-5 is still faster than in the physical mixture of ZSM-5 and  $\text{SiO}_2$ . Therefore, compared with traditional mechanical mixtures, the micropores and mesopore regions in Meso-ZSM-5 may be closer and have better connectivity, which is beneficial to the diffusion and exchange of xenon atoms. This study reveals the importance of pore connectivity in enhancing mass transfer within molecular sieves.

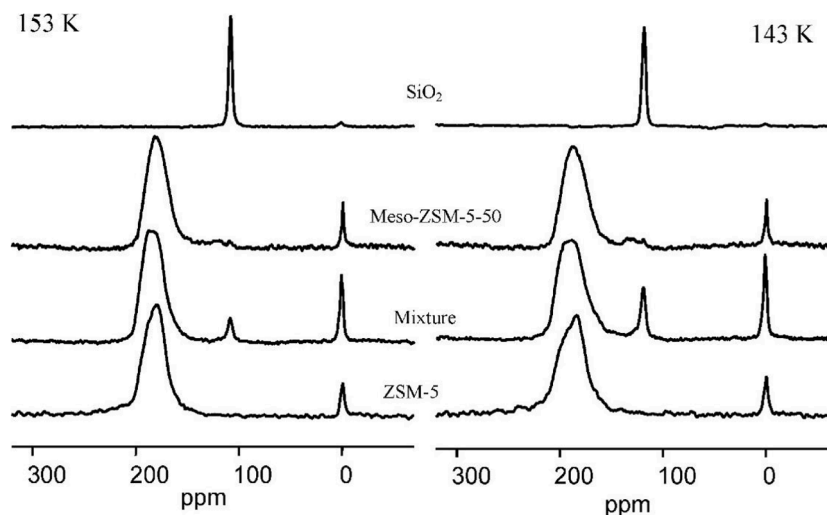


**Fig. 10.** HP  $^{129}\text{Xe}$  NMR spectra of xenon in  $\text{SiO}_2$ , Meso-ZSM-5, mechanical mixture ZSM-5/ $\text{SiO}_2$  and conventional ZSM-5 recorded at temperatures of 153 and 143 K, respectively [27].

Chen et al. [66] investigated the connectivity of pore systems for hierarchically micro-meso-macroporous Zr-doped silicalite-1 (MMM-ZrS-1) zeolite materials using HP  $^{129}\text{Xe}$  NMR. The findings display that even at a very low temperature of 143 K, the signal of xenon adsorbed in mesopores is difficult to detect in HP  $^{129}\text{Xe}$  NMR spectra. This indicates that xenon exchange quickly between mesopores and micropores, suggesting that the MMM-ZrS-1 exhibits excellent connectivity between these two types of pores.

### 3.6. Adsorption and diffusion in molecular sieve catalysis

In the catalytic reactions and separation processes of molecular sieves, the confined space formed by the pore or cage structure of a molecular sieve catalyst is not only a microreactor for a reaction but also an important channel for mass transfer. Many studies on heterogeneous catalytic reactions, such as MTO and DME carbonylation, have also pointed out the importance of research on the adsorption properties and mass transfer behavior of product molecules inside the pores of molecular sieves for the insight into the distribution of products and catalyst deactivation [7]. Although intensive studies have been conducted over the past decades, the establishment of structure-diffusion-activity relationships in molecular sieve catalysts has remained challenging.

Gao et al. [67] studied the mass transfer properties of SAPO-34 catalysts using HP  $^{129}\text{Xe}$  NMR and  $^1\text{H}$  PFG NMR techniques during the MTO reaction. The results of HP  $^{129}\text{Xe}$  NMR display that the formation and accumulation of carbon deposits within the CHA cage led to a sharp decrease in the volume of contactable micropores of the SAPO-34 catalyst. Furthermore,  $^1\text{H}$  PFG NMR reveals a rapid decrease in the intracrystalline self-diffusion coefficient of methane within the spent SAPO-34 catalyst, along with an increase in the activation energy for diffusion, as carbon deposition form within the pores, especially during the later stages of the MTO process. This means that in severely deactivated catalysts, the blockage of windows and occupation of cage structure by carbon deposition occur, and the mass transport of reactants and products within the crystal is extremely limited. According to the findings of the catalytic reaction, the deactivation mechanism of MTO catalyzed by SAPO-34 molecular sieve was supplemented from the aspects of the types and spatial distribution of carbon deposition and the impact of the formation of coke species on molecular transport and acidity of the catalyst.

Dai et al. [8] investigated the diffusion properties of ethane and ethylene within the SAPO-34 molecular sieve at various MTO reaction times using  $^1\text{H}$  PFG NMR, respectively. The diffusion studies reveal that

the decrease of effective pore size caused by carbon deposition formed in the pores of SAPO-34 resulted in a gradual decrease in the self-diffusion coefficients of ethane and ethylene as the MTO conversion increases, respectively. Meanwhile, the diffusion selectivity, defined as  $D_{\text{ethene}}/D_{\text{ethane}}$ , increases with the increase of MTO reaction time, which is one of the factors for the change in product distribution during the MTO reaction.

The role of two channels of MOR zeolite in the DME carbonylation combined with  $^1\text{H}$  PFG NMR and  $^{129}\text{Xe}$  NMR was explored by He et al. [68]. In the  $^1\text{H}$  PFG NMR experiment, using methane as a probe molecule, the results show that the self-diffusion coefficient of methane reduced from  $3.70 \times 10^{-9} \text{ m}^2\text{s}^{-1}$  for unmodified MOR to  $1.34 \times 10^{-9} \text{ m}^2\text{s}^{-1}$  for MOR modified by a certain amount of pyridine due to the blockage of 12 MR channel of MOR by pyridine, and the induction period of catalytic reaction increased from 260 to 420 min. However, the lifetime of the MOR zeolite was prolonged. Moreover, the NMR peak of adsorbed xenon located in the 8 MR side pocket of MOR zeolite modified by more pyridine could not be observed in  $^{129}\text{Xe}$  NMR spectra because of the complete blockage of the 12 MR by pyridine at 213–383 K, which indicates that xenon atoms could only diffuse into the 8 MR through the 12 MR. Based on the catalytic reaction analysis and NMR characterizations, it reveals that the 12 MR channel of MOR is an important passage for reactants to enter the active center located in the 8 MR and for the products to diffuse into the gas phase.

## 4. Conclusion

Exploring the adsorption property and diffusion efficiency of guest molecules within molecular sieves from the micro-scale is extremely significant for the optimization of catalyst and the exploration of the catalytic reaction mechanism. Based on the advanced NMR technology, the research progress in adsorption and diffusion of guest molecules within molecular sieves was summarized from the aspects of topology and pore distribution of molecular sieves and selective adsorption. The adsorption and mass transfer mechanisms of guest molecules within molecular sieves are closely related to the characteristics of pore structure.  $^{129}\text{Xe}$  NMR and HP  $^{129}\text{Xe}$  NMR exhibit unique benefits for assessing the pore structure, pore connectivity, and the location of different adsorption sites in molecular sieves. PFG NMR can evaluate the transport properties of adsorbed molecules within microporous and hierarchical molecular sieve materials at the microscopic level, which offers valuable diffusion evaluation for the development and optimization of catalysts.

With the advancements in science and technology, as well as the progress of NMR technology, the utilization of NMR in the research of adsorption and diffusion of guest molecules with multi-component in molecular sieves in-situ catalytic reaction at high-temperature should be paid more attention, which will provide deeper insights for the understanding of catalytic reaction mechanism.

### CRedit authorship contribution statement

**Shushu Gao:** Writing – review & editing, Writing – original draft, Conceptualization. **Jiamin Yuan:** Formal analysis. **Fangxiu Ye:** Writing – review & editing, Formal analysis. **Zhiqiang Liu:** Writing – review & editing, Formal analysis. **Anming Zheng:** Writing – review & editing, Funding acquisition, Conceptualization. **Shutao Xu:** Writing – review & editing, Funding acquisition, Conceptualization.

### Declaration of competing interest

The authors declare that they have no known competing financial interests or personal relationships that could have appeared to influence the work reported in this paper.

### Acknowledgments

This work was supported by the National Key Research and Development Program of China (No. 2022YFE0116000), the National Natural Science Foundation of China (22241801, 22022202, 22032005, 21972142, 21991090, 21991092), Dalian Outstanding Young Scientist Foundation (2021RJ01).

### Data availability

Data will be made available on request.

### References

- [1] M. Dusselier, M.E. Davis, Small-pore zeolites: synthesis and catalysis, *Chem. Rev.* 118 (2018) 5265–5329.
- [2] M. Moliner, C. Martínez, A. Corma, Multipore zeolites: synthesis and catalytic applications, *Angew. Chem. Int. Ed.* 54 (2015) 3560–3579.
- [3] P. Tian, Y.X. Wei, M. Ye, Z.M. Liu, Methanol to olefins (MTO): from fundamentals to commercialization, *ACS Catal.* 5 (2015) 1922–1938.
- [4] E.T.C. Vogt, B.M. Weckhuysen, Fluid catalytic cracking: recent developments on the grand old lady of zeolite catalysis, *Chem. Soc. Rev.* 44 (2015) 7342–7370.
- [5] D. Schneider, D. Mehlhorn, P. Zeigermann, J. Kärger, R. Valiullin, Transport properties of hierarchical micro-mesoporous materials, *Chem. Soc. Rev.* 45 (2016) 3439–3467.
- [6] J. Kärger, Transport phenomena in nanoporous materials, *ChemPhysChem* 16 (2015) 24–51.
- [7] W. Zhang, S. Lin, Y. Wei, P. Tian, M. Ye, Z. Liu, Cavity-controlled methanol conversion over zeolite catalysts, *Natl. Sci. Rev.* 10 (2023) nwad120.
- [8] W. Dai, M. Scheibe, L.D. Li, N.J. Guan, M. Hunger, Effect of the methanol-to-olefin conversion on the PFG NMR self-diffusivities of ethane and ethene in large-crystalline SAPO-34, *J. Phys. Chem. C* 116 (2012) 2469–2476.
- [9] C. Chmelik, J. Kärger, In situ study on molecular diffusion phenomena in nanoporous catalytic solids, *Chem. Soc. Rev.* 39 (2010) 4864–4884.
- [10] J. Kärger, D.M. Ruthven, D.N. Theodorou, *Diffusion in Nanoporous Materials*, Wiley-VCH, Weinheim, 2012.
- [11] Q. Zhang, T.M. Wu, C. Chen, S. Mukamel, W. Zhuang, Molecular mechanism of water reorientational slowing down in concentrated ionic solutions, *Proc. Natl. Acad. Sci.* 114 (2017) 10023–10028.
- [12] P. Bai, E. Haldoupis, P.J. Dauenhauer, M. Tsapatsis, J.I. Siepmann, Understanding diffusion in hierarchical zeolites with house-of-cards nanosheets, *ACS Nano* 10 (2016) 7612–7618.
- [13] E. Weiland, M.-A. Springuel-Huet, A. Nossor, A. Gédéon, <sup>129</sup>Xenon NMR: review of recent insights into porous materials, *Microporous Mesoporous Mater.* 225 (2016) 41–65.
- [14] B. Fan, S. Xu, Y. Wei, Z. Liu, Progresses of hyperpolarized <sup>129</sup>Xe NMR application in porous materials and catalysis, *Magn. Reson. Lett.* 1 (2021) 11–27.
- [15] Z. Qin, K.A. Cychoz, G. Melinte, H. El Siblani, J.-P. Gilson, M. Thommes, C. Fernandez, S. Mintova, O. Ersen, V. Valtchev, Opening the cages of Faujasite-type zeolite, *J. Am. Chem. Soc.* 139 (2017) 17273–17276.
- [16] Y.X. Ma, Z.J. Li, L. Wei, S.Y. Ding, Y.B. Zhang, W. Wang, A dynamic three-dimensional covalent organic framework, *J. Am. Chem. Soc.* 139 (2017) 4995–4998.
- [17] S. Komulainen, J. Roukala, V.V. Zhivonitko, M.A. Javed, L.J. Chen, D. Holden, T. Hasell, A. Cooper, P. Lantto, V.V. Telkki, Inside information on xenon adsorption in porous organic cages by NMR, *Chem. Sci.* 8 (2017) 5721–5727.
- [18] F. Bloch, W.W. Hansen, M. Packard, Nuclear Induction, *Phys. Rev.* 69 (1946) 127.
- [19] E.M. Purcell, H.C. Torrey, R.V. Pound, Resonance absorption by nuclear magnetic moments in a solid, *Phys. Rev.* 69 (1946) 37–38.
- [20] I. Yarulina, A.D. Chowdhury, F. Meirer, B.M. Weckhuysen, J. Gascon, Recent trends and fundamental insights in the methanol-to-hydrocarbons process, *Nat. Catal.* 1 (2018) 398–411.
- [21] P.J. Barrie, J. Klinowski, <sup>129</sup>Xe NMR As a probe for the study of microporous solids: a critical review, *Prog. Nucl. Magn. Reson. Spectrosc.* 24 (1992) 91–108.
- [22] J.-L. Bonardet, J. Fraissard, A. Gédéon, M.-A. Springuel-Huet, Nuclear magnetic resonance of physisorbed <sup>129</sup>Xe used as a probe to investigate porous solids, *Catal. Rev. Sci. Eng.* 41 (1999) 115–225.
- [23] E. Brun, J. Oeser, H.H. Staub, C.G. Telschow, The nuclear magnetic moments of <sup>129</sup>Xe and <sup>131</sup>Xe, *Phys. Rev.* 93 (1954) 904.
- [24] T. Ito, J. Fraissard, <sup>129</sup>Xe NMR study of xenon adsorbed on Y zeolites, *J. Chem. Phys.* 76 (1982) 5225–5229.
- [25] J. Demarquay, J. Fraissard, <sup>129</sup>Xe NMR of xenon adsorbed on zeolites: relationship between the chemical shift and the void space, *Chem. Phys. Lett.* 136 (1987) 314–318.
- [26] A. Nossor, F. Guenneau, M.-A. Springuel-Huet, E. Haddad, V. Montouillout, B. Knott, F. Engelke, C. Fernandez, A. Gedeon, Continuous flow hyperpolarized <sup>129</sup>Xe-MAS NMR studies of microporous materials, *Phys. Chem. Chem. Phys.* 5 (2003) 4479–4483.
- [27] Y. Liu, W. Zhang, Z. Liu, S. Xu, Y. Wang, Z. Xie, X. Han, X. Bao, Direct observation of the mesopores in ZSM-5 zeolites with hierarchical porous structures by laser-hyperpolarized <sup>129</sup>Xe NMR, *J. Phys. Chem. C* 112 (2008) 15375–15381.
- [28] S.T. Xu, W.P. Zhang, X.C. Liu, X.W. Han, X.H. Bao, Enhanced in situ continuous-flow mas NMR for reaction kinetics in the nanocages, *J. Am. Chem. Soc.* 131 (2009) 13722–13727.
- [29] W. Zhang, S. Xu, X. Han, X. Bao, In situ solid-state NMR for heterogeneous catalysis: a joint experimental and theoretical approach, *Chem. Soc. Rev.* 41 (2012) 192–210.
- [30] S.R. Schaefer, G.D. Cates, T.-R. Chien, D. Gonatas, W. Happer, T.G. Walker, Frequency shifts of the magnetic-resonance spectrum of mixtures of nuclear spin-polarized noble gases and vapors of spin-polarized alkali-metal atoms, *Phys. Rev. A* 39 (1989) 5613–5623.
- [31] D. Raftery, H. Long, T. Meersmann, P.J. Grandinetti, L. Reven, A. Pines, High-field NMR of adsorbed xenon polarized by laser pumping, *Phys. Rev. Lett.* 66 (1991) 584–587.
- [32] X. Zeng, C. Wu, M. Zhao, S. Li, L. Li, X. Zhang, Z. Liu, W. Liu, Laser-enhanced low-pressure gas NMR signal from <sup>129</sup>Xe, *Chem. Phys. Lett.* 182 (1991) 538–540.
- [33] W. Happer, E. Miron, S. Schaefer, D. Schreiber, W.A. van Wijngaarden, X. Zeng, Polarization of the nuclear spins of noble-gas atoms by spin exchange with optically pumped alkali-metal atoms, *Phys. Rev. A* 29 (1984) 3092–3110.
- [34] B.M. Goodson, Nuclear magnetic resonance of laser-polarized noble gases in molecules, materials, and organisms, *J. Magn. Reson.* 155 (2002) 157–216.
- [35] J. Jeener, B.H. Meier, P. Bachmann, R.R. Ernst, Investigation of exchange processes by two-dimensional NMR spectroscopy, *J. Chem. Phys.* 71 (1979) 4546–4553.
- [36] I.L. Moudrakovski, C.I. Ratcliffe, J.A. Ripmeester, Application of <sup>129</sup>Xe 2D-EXSY NMR to intra- and interparticle exchange in zeolites, *Appl. Magn. Reson.* 8 (1995) 385–399.
- [37] C.S. Johnson Jr, Diffusion ordered nuclear magnetic resonance spectroscopy: principles and applications, *Prog. Nucl. Magn. Reson. Spectrosc.* 34 (1999) 203–256.
- [38] R.M. Cotts, M.J.R. Hoch, T. Sun, J.T. Markert, Pulsed field gradient stimulated echo methods for improved NMR diffusion measurements in heterogeneous systems, *J. Magn. Reson.* 83 (1989) 252–266.
- [39] A.C. Forse, M.I. Gonzalez, R.L. Siegelman, V.J. Witherspoon, S. Jawahery, R. Mercado, P.J. Milner, J.D. Martell, B. Smit, B. Blümich, J.R. Long, J.A. Reimer, Unexpected diffusion anisotropy of carbon dioxide in the metal-organic framework Zn<sub>2</sub>(dobpdc), *J. Am. Chem. Soc.* 140 (2018) 1663–1673.
- [40] J. Kärger, H. Pfeifer, F. Stallmach, N.N. Feoktistova, S.P. Zhdanov, <sup>129</sup>Xe and <sup>13</sup>C PFG NMR study of the intracrystalline self-diffusion of Xe, CO<sub>2</sub>, and CO, *Zeolites* 13 (1993) 50–55.
- [41] C. D'Agostino, M.D. Mantle, C.L. Mullan, C. Hardacre, L.F. Gladden, Diffusion, ion pairing and aggregation in 1-ethyl-3-methylimidazolium-based ionic liquids studied by <sup>1</sup>H and <sup>19</sup>F PFG NMR: effect of temperature, anion and glucose dissolution, *ChemPhysChem* 19 (2018) 1081–1088.
- [42] D. Freude, N. Dvoyashkina, S.S. Arzumanov, D.I. Kolokolov, A.G. Stepanov, C. Chmelik, H. Jin, Y.S. Li, J. Kärger, J. Haase, NMR study of the host structure and guest dynamics investigated with alkane/alkene mixtures in metal organic frameworks ZIF-8, *J. Phys. Chem. C* 123 (2019) 1904–1912.
- [43] N. Dvoyashkina, D. Freude, A.G. Stepanov, W. Böhlmann, R. Krishna, J. Kärger, J. Haase, Alkane/alkene mixture diffusion in silicalite-1 studied by MAS PFG NMR, *Microporous Mesoporous Mater.* 257 (2018) 128–134.
- [44] E.O. Stejskal, J.E. Tanner, Spin Diffusion Measurements: spin Echoes in the Presence of a Time-Dependent Field Gradient, *J. Chem. Phys.* 42 (1965) 288–292.
- [45] J.E. Tanner, Use of the stimulated echo in NMR diffusion studies, *J. Chem. Phys.* 52 (1970) 2523–2526.
- [46] D. Mehlhorn, A. Inayat, W. Schwiager, R. Valiullin, J. Kärger, Probing mass transfer in mesoporous faujasite-type zeolite nanosheet assemblies, *ChemPhysChem* 15 (2014) 1681–1686.

- [47] J. Yuan, Z. Liu, Y. Wu, J. Han, X. Tang, C. Li, W. Chen, X. Yi, J. Zhou, R. Krishna, G. Sastre, A. Zheng, Thermal resistance effect on anomalous diffusion of molecules under confinement, *Proc. Natl. Acad. Sci. U.S.A.* 118 (2021) e2102097118.
- [48] Z.Q. Liu, X.F. Yi, G.R. Wang, X.M. Tang, G.C. Li, L. Huang, A.M. Zheng, Roles of 8-ring and 12-ring channels in mordenite for carbonylation reaction: from the perspective of molecular adsorption and diffusion, *J. Catal.* 369 (2019) 335–344.
- [49] S. Gao, S. Xu, Y. Wei, Z. Liu, A. Zheng, P. Wu, Z. Liu, Direct probing of heterogeneity for adsorption and diffusion within a SAPO-34 crystal, *Chem. Commun.* 55 (2019) 10693–10696.
- [50] S. Gao, J. Yuan, Z. Liu, C. Lou, Z. Yu, S. Xu, A. Zheng, P. Wu, Y. Wei, Z. Liu, Correlating the adsorption preference and mass transfer of xenon in RHO-type molecular sieves, *J. Phys. Chem. C* 125 (2021) 6832–6838.
- [51] M.G. Samant, L.C. Demenoral, R.A.D. Betta, M. Boudart, Nuclear magnetic resonance of xenon occluded in Na-A zeolite, *J. Phys. Chem.* 92 (1988) 3937–3938.
- [52] R.G. Larsen, J. Shore, K. Schmidt-Rohr, L. Emsley, H. Long, A. Pines, NMR study of xenon dynamics and energetics in Na-A zeolite *Chem. Phys. Lett.* 214 (1993) 220–226.
- [53] C.J. Jameson, A.K. Jameson, R. Gerald, A.C. de Dios,  $^{129}\text{Xe}$  nuclear magnetic resonance studies of xenon in zeolite CaA, *J. Chem. Phys.* 96 (1992) 1690–1697.
- [54] K. Gong, F. Jiao, Y. Chen, X. Liu, X. Pan, X. Han, X. Bao, G. Hou, Insights into the site-selective adsorption of methanol and water in mordenite zeolite by  $^{129}\text{Xe}$  NMR spectroscopy, *J. Phys. Chem. C* 123 (2019) 17368–17374.
- [55] J. Feng, P. Xiulian, G. Ke, C. Yuxiang, L. Gen, B. Xinhe, Shape-selective zeolites promote ethylene formation from syngas via a ketene intermediate, *Angew. Chem. Int. Ed.* 57 (2018) 4692–4696.
- [56] Z. Qin, S. Zeng, G. Melinte, T. Bućko, M. Badawi, Y. Shen, J.-P. Gilson, O. Ersen, Y. Wei, Z. Liu, X. Liu, Z. Yan, S. Xu, V. Valtchev, S. Mintova, Understanding the fundamentals of microporosity upgrading in zeolites: increasing diffusion and catalytic performances, *Adv. Sci.* 8 (2021) 2100001.
- [57] F. Chen, F. Deng, M. Cheng, Y. Yue, C. Ye, X. Bao, Preferential occupation of xenon in zeolite MCM-22 as revealed by  $^{129}\text{Xe}$  NMR spectroscopy, *J. Phys. Chem. B* 105 (2001) 9426–9432.
- [58] V. Gupta, S.S. Nivarthi, A.V. McCormick, H.Ted Davis, Evidence for single file diffusion of ethane in the molecular sieve  $\text{AlPO}_4\text{-5}$ , *Chem. Phys. Lett.* 247 (1995) 596–600.
- [59] H. Jobic, A. Méthivier, G. Ehlers, B. Farago, W. Haeussler, Accelerated diffusion of long-chain alkanes between nanosized cavities, *Angew. Chem. Int. Ed.* 43 (2004) 364–366.
- [60] S. Zeng, S. Xu, S. Gao, M. Gao, W. Zhang, Y. Wei, Z. Liu, Differentiating diffusivity in different channels of ZSM-5 Zeolite by pulsed field gradient (PFG) NMR, *ChemCatChem* 12 (2020) 463–468.
- [61] A. Ghysels, S.L.C. Moors, K. Hemelsoet, K. De Wispelaere, M. Waroquier, G. Sastre, V. Van Speybroeck, Shape-selective diffusion of olefins in 8-Ring solid acid microporous zeolites, *J. Phys. Chem. C* 119 (2015) 23721–23734.
- [62] S. Gao, Z. Liu, S. Xu, A. Zheng, P. Wu, B. Li, X. Yuan, Y. Wei, Z. Liu, Cavity-controlled diffusion in 8-membered ring molecular sieve catalysts for shape selective strategy, *J. Catal.* 377 (2019) 51–62.
- [63] M.-H. Sun, S.-S. Gao, Z.-Y. Hu, T. Barakat, Z. Liu, S. Yu, J.-M. Lyu, Y. Li, S.-T. Xu, L.-H. Chen, B.-L. Su, Boosting molecular diffusion following the generalized Murray's Law by constructing hierarchical zeolites for maximized catalytic activity, *Natl. Sci. Rev.* 9 (2022) nwac236.
- [64] P. Peng, X.-H. Gao, Z.-F. Yan, S. Mintova, Diffusion and catalyst efficiency in hierarchical zeolite catalysts, *Natl. Sci. Rev.* 7 (2020) 1726–1742.
- [65] A. Galarneau, F. Guenneau, A. Gedeon, D. Mereib, J. Rodriguez, F. Fajula, B. Coasne, Probing interconnectivity in hierarchical microporous/mesoporous materials using adsorption and nuclear magnetic resonance diffusion, *J. Phys. Chem. C* 120 (2016) 1562–1569.
- [66] L.-H. Chen, S.-T. Xu, X.-Y. Li, G. Tian, Y. Li, J.C. Rooke, G.-S. Zhu, S.-L. Qiu, Y.-X. Wei, X.-Y. Yang, Z.-M. Liu, B.-L. Su, Multimodal Zr-Silicalite-1 zeolite nanocrystal aggregates with interconnected hierarchically micro-meso-macroporous architecture and enhanced mass transport property, *J. Colloid Interface Sci.* 377 (2012) 368–374.
- [67] S.S. Gao, S.T. Xu, Y.X. Wei, Q.L. Qiao, Z.C. Xu, X.Q. Wu, M.Z. Zhang, Y.L. He, S. L. Xu, Z.M. Liu, Insight into the deactivation mode of methanol-to-olefins conversion over SAPO-34: coke, diffusion, and acidic site accessibility, *J. Catal.* 367 (2018) 306–314.
- [68] T. He, X. Liu, S. Xu, X. Han, X. Pan, G. Hou, X. Bao, Role of 12-ring channels of mordenite in DME carbonylation investigated by solid-state NMR, *J. Phys. Chem. C* 120 (2016) 22526–22531.